

Frontier Shepherding: A Bio-Mimetic Multi-robot Framework for Large-Scale Exploration

John Lewis¹, Meysam Basiri¹, and Pedro U. Lima¹

Abstract—Efficient exploration of large-scale environments remains a critical challenge in robotics, with applications ranging from environmental monitoring to search and rescue operations. This article proposes a bio-mimetic multi-robot framework, *Frontier Shepherding (FroShe)*, for large-scale exploration. The presented bio-inspired framework heuristically models frontier exploration similar to the herding behavior of herding dogs. This is achieved by modeling frontiers as a sheep swarm reacting to robots modeled as herding dogs. The framework is robust across varying environment sizes and obstacle densities and can be easily deployed across multiple agents. Simulation results showcase that the proposed method consistently performed irrespective of the simulated environment’s varying sizes and obstacle densities. With the increase in the number of agents, the proposed method outperforms other state-of-the-art exploration methods, with an average improvement of 20% with the next-best approach (for 3 UAVs). The proposed technique was implemented and tested in a single and dual drone scenario in a real-world forest-like environment.

I. INTRODUCTION

Robotic applications involving exploration or surveillance of a large-scale area can be taxing for a single robot. Delegation of such tasks across multiple robots improves overall efficiency. However, multi-robot solutions often require prior planning, training, or optimization techniques to improve coordination, minimize overlapped exploration, and overcome communication constraints. Such planning might be complex in scenarios such as search and rescue, disaster response, and large-scale exploration of unknown, unstructured areas. Quick and robust deployment of multiple robots for such scenarios while ensuring complete coverage is thus vital.

A. Related Work

Fast and robust autonomous exploration is an essential aspect of outdoor robotics, crucially to achieve complete autonomy in scenarios such as search and rescue [1], disaster response [2], and mapping of large-scale unknown areas [3]. A conventional autonomous exploration task is carried out by defining *frontiers* [4] as the boundary between the known/mapped and unknown/unmapped areas. Exploration is achieved by pushing this boundary or mathematically by

minimizing the perimeter or length of the frontier. However, this straightforward solution renders inadequate and increasingly complex in the presence of obstacles, energy and time constraints, and completeness of the exploration. Thus, prioritizing viewpoints from the knowledge of frontier, the path planned and the perception sensor can optimize the flight time required for exploration [3–5], where viewpoints are the points at which the frontier can be altered.

Frontier exploration strategies include greedy exploration [6], proximal exploration [7] or exploration based on prior training [8]. Proximal exploration strategies require conditional supervision to prevent the robot from being stuck in local minima. In contrast, greedy exploration strategies can often lead to sub-par time management, especially in highly cluttered environments. Deep learning or reinforcement learning strategies require prior training and substantial data, resulting in slow deployment. Furthermore, reliance on training on extensive data may not capture the complexities of unforeseen environments. Fast deployment is crucial in disaster response and search and rescue scenarios. Markov decision process (MDP) based exploration strategies [9–11] often guarantee safety but can be computationally intensive.

Increasing the speed of exploration robots may offer benefits in terms of time efficiency but introduces several challenges. These include increased collision risks, limitations in perception and sensing, control and stability issues, and the need for faster data processing and communication. An alternative solution would be segregating the overall exploration task across multiple robots. Over the years, multi-agent exploration solutions have improved from a general strategy [12, 13] to tackle specific exploration tasks such as forests [3], caves [14] and indoors [15]. Bartolomei et al. [3] enhances exploration by utilizing a dual mode, namely explorer and collector. In explorer, the agents push the frontiers, and in collector, the “trails” or leftover unknown pockets are explored. The dual mode enables a variable velocity, with a higher velocity in collector mode to capture the “trails” faster, thereby guaranteeing speed and safety.

An uncoordinated multi-agent system can often lead to multiple sweeps of the same area to achieve complete coverage. Thus, communication and coordination are vital to extract the full effectiveness of a multi-robot system. This requirement increases complexity with the increase in number of robots. In a communication-constrained scenario, Yuman Gao et al. [16] proposed a framework where the agents initially coordinate a meeting point to share the map. The agents then explore an area and reconvene at the predetermined meeting point to merge maps and determine

* This work was supported by doctoral grant from Fundação para a Ciência e a Tecnologia (FCT) UI/BD/153758/2022, Aero.Next project (PRR - C645727867- 00000066) and ISR/LARSyS Strategic Funding through the FCT project DOI: 10.54499/UIDB/50009/2020, DOI: 10.54499/UIDP/50009/2020, DOI: 10.54499/LA/P/0083/2020

¹J. Lewis, M. Basiri and P. Lima are with the Institute for Systems and Robotics, Instituto Superior Técnico, Universidade de Lisboa, Lisbon 1049-001, Portugal (e-mail: {john.lewis; meysam.basiri; pedro.lima}@tecnico.ulisboa.pt).

Video: <https://youtu.be/Kme95Bf8ros>

the meeting points and areas to explore. In bandwidth-constrained instances, sparse information can be transmitted over a long-range communication protocol, and complete information transfer can be instigated utilizing a short-range communication protocol. In such scenarios, the method proposed by Lewis et al. [17] enables sharing minimal point-cloud, and GNSS coordinates over long-range communication, while short-range communication is used for sharing a complete map. This minimal information can assist in exploration as the robots are clued in on the possible explored areas. A coordinated exploration utilizing a decentralized approach by relying on point-to-point communication [18] ensures that the agents are spread out, thereby minimizing the overlap with previously explored areas of other agents.

Naturally occurring behaviors such as sheep herding [19], ant foraging [20], and fish swarming [21] can be heuristically modeled to incorporate swarm-like behavior. These minimal heuristic inter-agent relations lead to emergent behaviors and can be used for rapid deployment and control of robotic swarms [22]. Additional swarm control can be attained by integrating heuristics into the agent behavior, which acts as a reaction to an external agent. The added change in swarm dynamics can be predatory [19, 23] or leader-like [24, 25], depending on the nature of the task at hand. The ability to control a large swarm of robots by manipulating a few robots is a favorable option as it minimizes the control, communication, and coordination requirements. In the context of exploration, prior works [25–27] have explored or can be extended to include exploration tasks utilizing swarms.

B. Contributions

In this article, we present Frontier Shepherding (*FroShe*), a novel bio-mimetic multi-robot framework for large-scale exploration. The proposed exploration framework, (i) utilizes heuristic bio-mimetism to explore frontiers; (ii) achieves frontier prioritization using virtual bio-mimetic agents and behavior; (iii) provides robust performances across varying environments and coverage areas. The proposed modular, online, and decentralized strategy enables robust and scalable exploration suitable for quickly deploying computationally constrained robot(s) for mapping unknown and hazardous terrains.

The article’s outline is as follows: Section II details the proposed multi-agent exploration framework. The experiments and results are presented in Section III. Finally, Section IV concludes the findings and pitches possible improvements to the proposed method.

II. METHODOLOGY

A team of n_r robots, $\mathcal{R} = [R_1 \dots, R_{n_r}]$, is tasked to explore and map an unknown environment of area, \mathcal{A} . The robots are equipped with a perception sensor (eg., Ouster, Depth sensors), with a perception range of L , to generate a terrain representation. The proposed methodology is broadly grouped into three stages, as shown in Fig. 1.

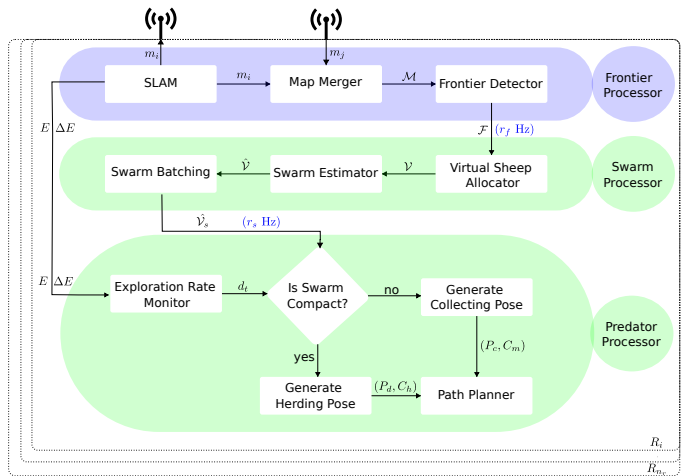


Fig. 1: The FroShe framework

A. Frontier Processor

Each $R_i \in \mathcal{R}$, with pose \bar{R}_i , runs a continuous onboard mapping algorithm [28–30] to generate and update its own map [31], m_i . In the absence of a global communication topology, a communication-constrained map merging algorithm [16, 17] is utilized to merge m_i with m_j ($\forall j \in [1, n_r], i \neq j$). The merged map, \mathcal{M} , is equivalent to the global view the whole team perceives. The set of n_f map frontiers, $\mathcal{F} = [f_1, f_2, \dots, f_{n_f}]$, in \mathcal{M} is calculated [32, 33]. \mathcal{F} and \mathcal{M} are continuously updated, at a rate of r_f Hz, throughout the exploration process. The modular framework of the frontier processor stage provides flexibility in choosing a specific method for the various building blocks depending on the communication constraints, robot parameters, and levels of cooperation required. Given the computationally intensive modules of SLAM, communication delays, map merging, and frontier detection, the output of the frontier processor is expected to be slow.

B. Swarm Processor

The Swarm Processor module heuristically models \mathcal{F} as a virtual sheep swarm at a rate of $r_s (>> r_f)$ Hz. In [19], the behavior of the sheep swarm is heuristically emergent from 5 forces, as represented in Table I. Out of these 5 forces, inertial, erroneous, and inter-agent repulsion forces consistently act upon each sheep, while clustering and predatory-response forces are triggered when a sheep is within the sphere of influence of a predator. Adapting to this emergent behavior of a sheep swarm, the shepherding dog’s behavior is heuristically modeled [19] to control the sheep swarm. The various forces involved in the heuristic model [19] for a swarm of n sheep, $\mathcal{S} = [S_1 \dots, S_n]$, in the presence of m shepherding dogs $\mathcal{P} = [P_1 \dots, P_m]$ is summarized in Table I. The heuristic predator model either collects or herds the sheep swarm depending upon the compactness of the swarm. h , ρ_a , c , and ρ_s are constants that determine the strength of each force that acts upon sheep S_i , with pose \bar{S}_i and shepherds’ pose \bar{P}_j . e is a small random erroneous number emulating noise in the swarm.

Force	on Sheep, S_i [19]	on virtual sheep, v_i
Inertial Force	$h\bar{S}_i(t)$	0
Inter-Agent Repulsive Force	$\rho_a \frac{(\bar{S}_i - \bar{S}_j)}{\ S_i - S_j\ }$	f_{res}
Erroneous Force	e	e
Clustering Force	$\frac{c}{n} \sum_{j=1, \neq i}^n \bar{S}_j$	$\frac{-c_f}{n} \sum_{j=1, \neq i}^{n_v} v_j$
Predatory Force	$\sum_{j=1}^m \frac{\rho_s}{\ P_j - \bar{S}_i\ }$	$\sum_{j=1}^{n_r} \frac{\rho_f}{\ R_j - v_i\ }$
Predator detection range	r_p	L

TABLE I: Modelling frontiers analogous to sheep swarm. The cumulative sum of the forces determines the behavior of the S_i and v_i .

A primary contribution of FroShe is modeling the frontiers of a map as sheep swarm and the exploration agents as shepherding dogs. The task of herding \mathcal{S} sheep with \mathcal{P} shepherding dogs in [19], is mimicked as a task of exploring frontier \mathcal{F} with team \mathcal{R} . This helps the robot estimate the frontier behavior when the output of the frontier processor is delayed. To successfully emulate shepherding dogs, the robots must perceive the frontiers as sheep swarm.

1) *Virtual Sheep Allocator*: The virtual sheep allocator converts the set of frontiers, \mathcal{F} , to a set of $n_v (< n_f)$ virtual sheep, $\mathcal{V} = [(v_1, w_1), (v_2, w_2), \dots, (v_{n_v}, w_{n_v})]$ with enumerated (pose, weight) tuples. In this module, R_i initializes a virtual sheep of unit weight for each detected frontier, $f_k \in \mathcal{F}$. The swarm processor module uses a resolution, f_{res} , to discretize continuous frontiers and reduce the initialized virtual sheep count. The virtual sheep falling within f_{res} of each other will be merged in terms of weight and moved to the center of mass of the sheep involved. This approach ensures that multiple frontiers within close proximity are weighed according to the exposed unexplored area of the combined frontiers. This also relates to inter-agent repulsive force [19], as no two virtual sheep can be closer than f_{res} . A simple 2D representation of the resultant map frontiers for a single robot and the allocated virtual sheep is shown in Fig. 2a and Fig. 2b, respectively.

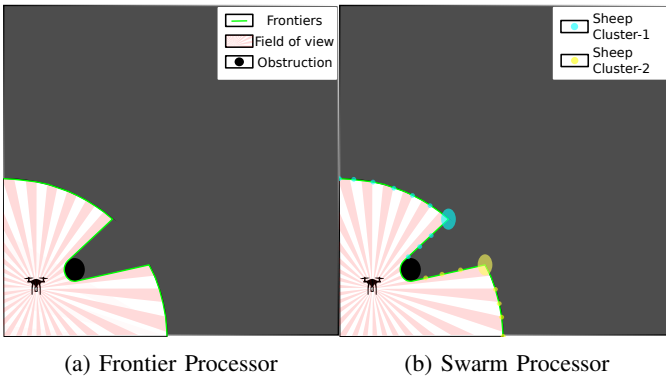


Fig. 2: Virtual sheep are represented by blobs, with the radius depicting the weight of each virtual sheep. The larger blob sizes at the corners portray multiple virtual sheep merging into one heavier virtual sheep.

2) *Swarm Estimator*: The swarm estimator estimates the behavior of \mathcal{V} as R_i moves through the terrain and generates the estimated swarm, $\hat{\mathcal{V}}$. This is done by modeling the forces of a sheep swarm with respect to the behavior of a frontier. The analogous forces are presented in Table I and explained below.

Unlike sheep, the frontiers do not have an inertial component, wherein the frontiers move in the previously traveled direction. Thus, we are equating the analogous frontier inertial force to 0. Erroneous force mimics the minor perturbations in the sheep swarm and is directly translated into our modeling.

The sphere of influence of R_i is the range, L , of the perception sensor. When a virtual sheep is within the sensory range, it activates the clustering and predatory response of the virtual sheep. The predatory response force is similar to [19]. The expected response of the sheep and frontiers, when in range of a predator/robot is to repel away. Along similar lines, we model the frontiers to disperse in the presence of a robot, thus the clustering force has a negative element to its shepherding counterpart.

This approach to modeling frontiers, \mathcal{F} , with a sheep swarm, \mathcal{V} , allows the subsequent shepherding module to heuristically estimate the next possible frontier by predicting the behavior of virtual sheep. When a new update of \mathcal{F} is acquired from the frontier processor, \mathcal{V} is updated and $\hat{\mathcal{V}}$ is reset to \mathcal{V} . The output of the swarm estimator, and eventually the swarm processor, is at a rate of $r_s \gg r_f$ Hz. The increased rate allows the swarm processor to act as a buffer between the frontier and the predator processor modules. This ensures plausible delays from the frontier processor do not negatively impact the subsequent path planning.

3) *Swarm Batching*: $\hat{\mathcal{V}}$ can be discontinuous due to occlusions (Fig. 2b) and the dispersive nature of the swarm estimator (Fig. 3b and Fig. 4b). In such scenarios, considering the whole swarm as a single entity can lead to preventable inter-robot collision, chasing similar frontiers, and repeated path planning. In the swarm batching module, $\hat{\mathcal{V}}$ is segregated into n_b batches using a clustering algorithm [34]. Each cluster is described as a tuple (v_b, w_b) , where v_b is the center of mass of a cluster of $\hat{\mathcal{V}}$, and w_b is the corresponding cumulative weight of the cluster. The set of virtual sheep swarm cluster descriptors, $\mathcal{V}_b = [(v_{b1}, w_{b1}), (v_{b2}, w_{b2}), \dots, (v_{bn_b}, w_{bn_b})]$, is polled amongst \mathcal{R} .

Each tuple in \mathcal{V}_b uniquely maps to a cluster of sheep in $\hat{\mathcal{V}}$ or $\hat{\mathcal{V}}(\mathcal{V}_b(k))$ represents a unique sheep cluster, $\forall k \in [1, n_b]$. Exploring the batch of virtual sheep with the maximum cumulative weight is ideal for maximum exploration gain. We incorporate a distance penalty to ensure each agent prefers a closer swarm batch to prevent unwarranted switching between batches and multiple robots chasing the same frontiers. An allocated batch is removed from the poll and updated across the team, thus enforcing a one-to-one swarm batch to robot mapping. Each robot within proximity calculates the distance to each v_b and the corresponding weight. Normalization with respect to the maximum of both distance, d_{max} and weight, w_{max} is carried out to bound the values. Each robot, R_i chooses the cluster, $\hat{\mathcal{V}}_s = \hat{\mathcal{V}}(\mathcal{V}_b(B_i))$,

where B_i maximizes Eq. (1). The distance coefficient λ_d and the weight coefficient λ_m are tunable parameters that can be tuned according to the robotic team involved. For UAVs, a lower λ_d promises a reduced impact on distance in the maximization problem. For UGVs, traversing longer distances can be more taxing and thus increasing λ_d will favour nearby heavier batches.

$$B_i = \arg \max_{(v_b, w_b) \in \mathcal{V}_b} \left(\lambda_m \frac{m_b}{w_{max}} - \lambda_d \frac{\|\bar{R}_i - v_b\|_2}{d_{max}} \right) \quad (1)$$

C. Predator Processor

R_i 's swarm processor module (Sec.II-B) provides the selected subset of virtual sheep swarm, $\hat{\mathcal{V}}_s$, that is to be herded. A heuristic predator has two modes of operation: *collecting* and *herding* depending on the compactness of the sheep swarm. $\hat{\mathcal{V}}_s$ is deemed to be compact if all the sheep in $\hat{\mathcal{V}}_s$ is within a distance threshold, d_t from the center of mass of $\hat{\mathcal{V}}_s$, C_m . A global perception parameter, p_p , determines how closely R_i will approach to influence $\hat{\mathcal{V}}_s$. As the robot moves through the terrain, the estimates $\hat{\mathcal{V}}$ and $\hat{\mathcal{V}}_s$ change in congruence with the forces of Table I.

1) *Collecting*: When the swarm is not compact, a predator attempts to push the outlier sheep towards the center of mass, to keep the swarm compact. Analogously, a collecting pose P_c , formulated in Eq. (2), is generated close to the furthest sheep, v_f , in $\hat{\mathcal{V}}_s$. A trajectory is planned to P_c (Fig. 3a) and from P_c to C_m (Fig. 3b).

$$P_c = v_f + p_p * L * \frac{C_m - v_f}{\|C_m - v_f\|} \quad (2)$$

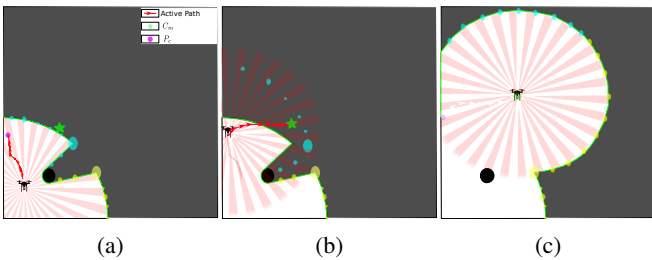


Fig. 3: Collecting mode. (a) Planned trajectory to P_c (b) Planned trajectory from P_c to C_m (c) Final \mathcal{F} in \mathcal{M} after collecting.

2) *Herding*: When the swarm is compact, the heuristic predator attempts to push the swarm to the desired destination. Since an exploration task is devoid of a destination, a driving pose P_d , as formulated in Eq. (3), is generated with respect to C_m of the current frontier batch and the center of mass of adjacent heaviest swarm batch, C_h . Inherently, the predator attempts to merge the two batches with the largest possible exploratory gain. P_d is formulated in Eq. (3), and a trajectory is planned to P_d (Fig. 4a) and from P_d to C_h (Fig. 4b).

$$P_d = C_m - p_p * L * \frac{C_m - C_h}{\|C_m - C_h\|} \quad (3)$$

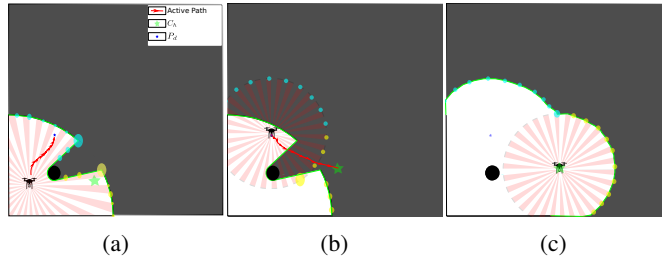


Fig. 4: Herding mode (a) Planned trajectory to P_d (b) Planned trajectory from P_d to C_h (c) Final \mathcal{F} in \mathcal{M} after herding.

Fig. 3b and Fig. 4b depicts the missing map update from the frontier processor. The figures also portray the effect of the swarm estimator in the absence of a map update.

3) *Exploration Rate Monitor*: In [19], a function of number of sheep, is used to determine the distance threshold, d_t . d_t defines the compactness of the sheep swarm. The swarm is compact if all agents are within d_t from the swarm's center of mass. Thus, a smaller d_t implies collecting would be the favorable strategy. Analogously, the reliance of d_t on frontier sizes can lead to degraded robustness to environments of varying features.

To ensure robustness, we monitor the the rate of change of percentage of explored area, ΔE , as a time series. The trend of ΔE is determined using a moving average model, $MA(n)$, with n depicting the rolling window size, represented in Eq. (4). $MA(n)$ model is an efficient tool to determine the overall trend of a time series used in scenarios varying from weather forecasting [35] to stock market prediction [36].

$$MA(n) = \frac{1}{n} \sum_{i=0}^{n-1} \Delta E_{t-i} \quad (4)$$

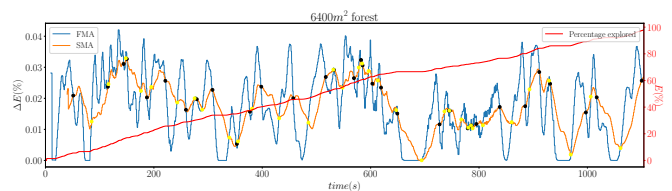


Fig. 5: Black and yellow dots represent the time instant from which d_t is changed and retained respectively.

For a given area, ΔE is always a positive change, i.e the moving averages are never negative. A slow moving average (SMA), when n is large (~ 200), depicts the overall trend of ΔE . A fast moving average (FMA), when n is small (~ 50) tracks the recent changes in the time series. A cause for concern occurs when FMA falls below SMA, implying that the recent exploration strategies have not resulted in meeting the long-term expected ΔE . We utilize this as flag to change the predator's strategy preferences, by tuning d_t . If the dominant strategy in the FMA time window is collecting, we increase d_t otherwise d_t is reduced to promote collecting. In

other words, d_t is changed, to prefer the strategy alternate to the current dominant one. When SMA falls below FMA, the recent strategies have been outperforming the expected ΔE , within the time window. This is used as a flag to use the current d_t , till FMA falls below SMA. Fig. 5, depicts a single-agent exploration scenario in a $6400m^2$ forest-like environment and various time instances at which the change in d_t is triggered. The auto-regressive moving average model tracks ΔE to tune d_t to ensure ΔE consistently meets the overall long-term expectation.

III. RESULTS

Section III-A provides an in-depth simulation analysis, carried out to compare the FroShe with SOTA multi-agent exploration strategies. Details of an implementation of the proposed algorithm in a real-world a forest-like scenario is showcased in Section III-B.

A. Simulation Results

1) *Setup*: Simulations are carried out in the MRS UAV system [37] on ROS Noetic, which provides an end-to-end multi-UAV framework complete with path planning enabled with collision avoidance and realistic-sensor integration along with various 3-D mapping algorithms [31, 38]. Additionally, [37] replicates realistic simulations that can be transferred to real-world implementation in a multi-UAV system.

The exploration methods are tested on 2 environments of varying degrees of obstacle clutter as shown in Fig. 6. We define $1600m^2$, $3600m^2$, and $6400m^2$ square patches for exploration in each environment to analyze the effect of varying areas of interest. The experiment is considered a failure if exploration is not completed within a predefined duration of 3600s. Results are analyzed across 25 runs with the drones spawned within 5m of each other, in one corner of the area of interest.

For the simulation setup, we simulate the agents as f550 UAVs enabled with an Ouster (OS1-128) LIDAR, with laser range limited to 10m. The maximum horizontal speed, maximum vertical speed, maximum acceleration and maximum jerk is limited to (4m/s, 2m/s, $2m/s^2$, $40m/s^3$) for grass plane and (1m/s, 1m/s, $1m/s^2$, $20m/s^3$) for forest, to ensure safety. The maximum allowed flight height is limited to 4m and the minimum is bounded at 1m. We utilize octomapping [31] to generate the 3-D map of the environment. The resultant local occupancy grid is globally shared across other UAVs.

The proposed algorithm is compared against FAME [3] and Burgard et al. [13] exploration algorithms. FAME provides a dual-mode approach to exploration incorporating a traveling salesman-based optimization. The algorithm, FAME¹, originally developed for a depth camera with a limited field of view, has been incorporated to include a 360° LIDAR. Burgard et al. approach explores with a utility-value function updated along the path to the target poses. The generated target poses are shared to MRS UAV



Fig. 6: Simulation Environments. (a) Grass plane: This environment is devoid of obstacles, allowing for straightforward path planning without obstacle avoidance. (b) Forest: This cluttered environment has an average tree density of 0.05 trees/ m^2 , providing a more challenging scenario for testing exploration strategies.

framework[37], to generate the trajectory after incorporating collision avoidance. No communication constraints are imposed on the agents.

2) *Analysis*: Fig. 7 shows the time box plots for a varying number of agents (1to3). Each subplot depicts a different combination of environment and area, with each bar plot representing FroShe, Burgard et al., Greedy exploration and FAME. FAME’s notable inconsistent performance deterioration with respect to what is reported in [3] could be attributed to the switch to the 360° LiDAR and switch to Gazebo simulator with Software-In-The-Loop (SITL) simulation, accurate sensor and actuator models, as well as realistic physics simulator and sensor noises. A much-needed ablation study of [3] with respect to FroShe is needed but is beyond the current article’s scope.

As expected and denoted in Fig. 7 and Fig. 8, there is a consistent improvement in total exploration time with the number of agents. However, the decrease in variance with the number of agents is more evident in FroShe, demonstrating that the proposed algorithm consistently covers the area within a given time. This consistency across all areas and environments demonstrates the robustness of the proposed algorithm compared to others.

Fig. 7 shows that, for a single agent scenario, both Burgard et al. and greedy strategies outperform frontier shepherding. The continuous switching between herding and collecting in a single agent scenario makes the proposed algorithm more time-consuming as more distance is to be covered for reduced exploration gain. However, as the number of agents increases, initial delegation of segregated frontier clusters (Sec II-A) via swarm allocation (Sec II-B.3) improves the efficiency of frontier shepherding. This reduces the expected distance travelled while switching between shepherding modes, thereby improving time taken. With 3 agents, we can see a average improvement of 25% in time-taken, with respect to the other approaches for all areas across all environments. It is also essential to point out that FAME performs best in $1600m^2$ forest, which could be attributed to the fact that the initial algorithm was tuned to suit a $2500m^2$ forest. To check the robustness and flexibility of each algorithm with minimal intervention, no parameters

¹https://github.com/VIS4ROB-lab/fast_multi_robot_exploration

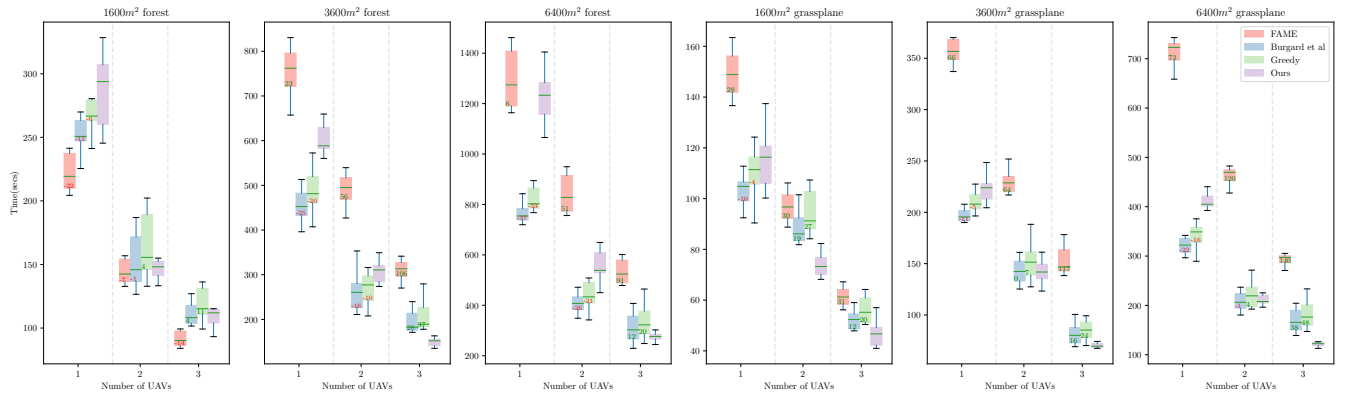


Fig. 7: Time-taken analysis for varying number of agents and varying area-environments for different exploration strategies. The numbers within the bars depict the percentage change with respect to the time taken by FroShe, with an **increase** or **decrease** in performance colored accordingly. Due to varying time taken across each subplot, it is to be noted that the time axis (in seconds) is not shared across the subplots.

were changed throughout the simulation analysis.

FroShe shows an evident improvement in the time taken, with respect to the other strategies, with the increase in the coverage area, with a minimum of 12% in forest and 48% in grass plane for a 3 agent scenario. The fast decline of overall exploration time with the increase in the number of UAVs is portrayed in Fig. 8. FAME was developed to explore forests and capture "trails" quickly. Thus, it was not expected to perform exceptionally in a no-obstacle course. The improvement is compared against FAME, both promising a consistent decline in flight time required to cover the area. The reduced variance in Fig. 8 showcases the robustness of FroShe.

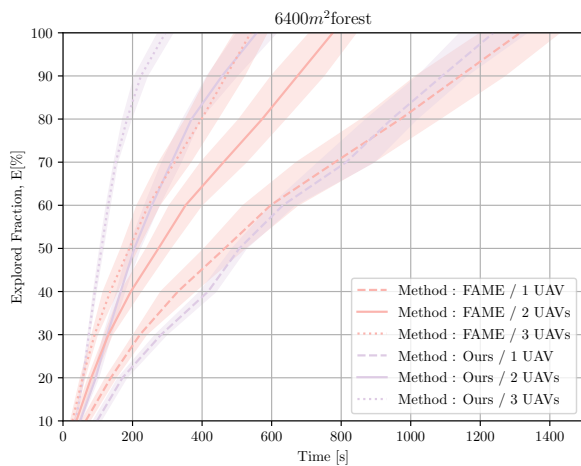


Fig. 8: Exploration rates over different numbers of UAVs for FroShe and FAME [3] in an $6400m^2$ forest.

B. Real World Experiments

The real-world experiments were carried out with the help of AeroSTREAM Open Remote Laboratory². We leveraged

²<https://fly4future.com/aerostream-open-remote-laboratory/>



Fig. 9: Real World Experiments with 2 X500 drones. The drones were separated by 10m.

the seamless integration of the MRS UAV framework [37] onto a real-world scenario in a forest-like environment, pictured in Fig. 9b. The experiments involved two X500 drones, shown in Fig. 9a, each equipped with an Ouster OS1 LiDAR. The experiments were conducted in a forest-like environment to generate a scenario that demands obstacle avoidance. Single UAV and dual UAV exploration experiments were conducted, with the UAV(s) tasked to explore a $400m^2$ and $600m^2$ area, with the lidar range clipped at 10m. The exploration trend for both experiments is showcased in Fig. 10.

IV. CONCLUSION

In this work, we propose *Frontier Shepherding (FroShe)*, a bio-mimetic multi-robot framework for large scale exploration. The proposed framework models frontiers as virtual sheep that is spread across the map. The multi-robot framework is then tasked to coordinate and collect and herd the virtual sheep, consequently exploring the environment. The heuristic approach to exploration ensures a fast deployment of robots and can be scaled to incorporate with minimal complexity. FroShe framework is tested in a forest and grass plane in simulations and a real-world execution is carried out in a forest patch. Results showcase a robust algorithm that is invariant to size or occlusion of the environment.

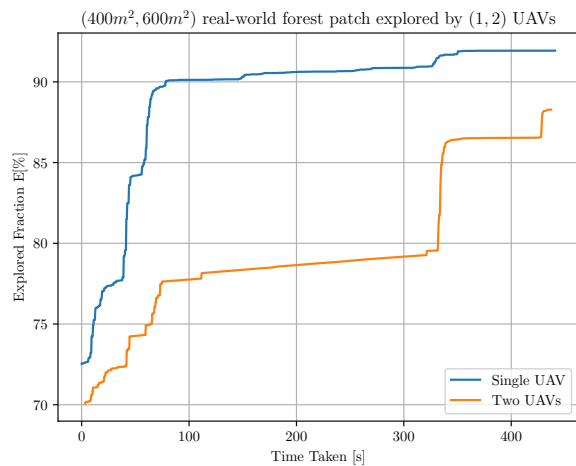


Fig. 10: Exploration rates over different numbers of UAVs exploring a real-world forest-like environment with FroShe. It is to be noted that for a 2 UAV scenario, the area of interest is 600m² and 400m² for 1 UAV scenario.

Furthermore, with the increase in the number of agents, FroShe is shown to outperform other SOTA exploration methods.

For future work, we aim to implement a heterogeneous team of robots that can utilize FroShe depending on each agent’s features. Similar to [3], a dual velocity approach to FroShe might improve its performance, specifically in a heterogeneous team. The current method employs an ego-centric exploration rate monitor that can be improved to incorporate the entire map, rather than the individual map. Such an approach can enable individual switching between herding and collecting based on collective performance and can improve collaboration.

V. ACKNOWLEDGEMENT

The authors would like to acknowledge all the help extended by the Multi-robot Systems (MRS) group at the Department of Cybernetics, Faculty of Electrical Engineering, of Czech Technical University in Prague. The support extended by the team helped acquire valuable real-world forest results.

REFERENCES

- [1] Meysam Basiri et al. “A multipurpose mobile manipulator for autonomous firefighting and construction of outdoor structures”. In: *Field Robot 1* (2021), pp. 102–126.
- [2] Payam Ghassemi and Souma Chowdhury. “Multi-robot task allocation in disaster response: Addressing dynamic tasks with deadlines and robots with range and payload constraints”. In: *Robotics and Autonomous Systems* 147 (2022), p. 103905.
- [3] Luca Bartolomei, Lucas Teixeira, and Margarita Chli. “Fast multi-UAV decentralized exploration of forests”. In: *IEEE Robotics and Automation Letters* (2023).
- [4] Andreas Bircher et al. “Receding horizon” next-best-view” planner for 3d exploration”. In: *2016 IEEE international conference on robotics and automation (ICRA)*. IEEE. 2016, pp. 1462–1468.
- [5] Qian-Yi Zhou, Jaesik Park, and Vladlen Koltun. “Fast global registration”. In: *European conference on computer vision*. Springer. 2016, pp. 766–782.
- [6] Daniel Duberg and Patric Jensfelt. “Ufoexplorer: Fast and scalable sampling-based exploration with a graph-based planning structure”. In: *IEEE Robotics and Automation Letters* 7.2 (2022), pp. 2487–2494.
- [7] Titus Cieslewski, Elia Kaufmann, and Davide Scaramuzza. “Rapid exploration with multi-rotors: A frontier selection method for high speed flight”. In: *2017 IEEE/RSJ International Conference on Intelligent Robots and Systems (IROS)*. IEEE. 2017, pp. 2135–2142.
- [8] Junyan Hu et al. “Voronoi-based multi-robot autonomous exploration in unknown environments via deep reinforcement learning”. In: *IEEE Transactions on Vehicular Technology* 69.12 (2020), pp. 14413–14423.
- [9] Matthew Budd et al. “Markov decision processes with unknown state feature values for safe exploration using gaussian processes”. In: *2020 IEEE/RSJ International Conference on Intelligent Robots and Systems (IROS)*. IEEE. 2020, pp. 7344–7350.
- [10] Fernando S Barbosa et al. “Risk-aware motion planning in partially known environments”. In: *2021 60th IEEE Conference on Decision and Control (CDC)*. IEEE. 2021, pp. 5220–5226.
- [11] Matthew Budd et al. “Bayesian reinforcement learning for single-episode missions in partially unknown environments”. In: *Conference on Robot Learning*. PMLR. 2023, pp. 1189–1198.
- [12] Wolfram Burgard et al. “Collaborative multi-robot exploration”. In: *Proceedings 2000 ICRA. Millennium Conference. IEEE International Conference on Robotics and Automation. Symposia Proceedings (Cat. No. 00CH37065)*. Vol. 1. IEEE. 2000, pp. 476–481.
- [13] Wolfram Burgard et al. “Coordinated multi-robot exploration”. In: *IEEE Transactions on robotics* 21.3 (2005), pp. 376–386.
- [14] Pavel Petráček et al. “Large-scale exploration of cave environments by unmanned aerial vehicles”. In: *IEEE Robotics and Automation Letters* 6.4 (2021), pp. 7596–7603.
- [15] Hui Lu et al. “Multi-robot indoor environment map building based on multi-stage optimization method”. In: *Complex System Modeling and Simulation* 1.2 (2021), pp. 145–161.
- [16] Yuman Gao et al. “Meeting-merging-mission: A multi-robot coordinate framework for large-scale communication-limited exploration”. In: *2022 IEEE/RSJ International Conference on Intelligent Robots and Systems (IROS)*. IEEE. 2022, pp. 13700–13707.

- [17] John Lewis, Pedro U Lima, and Meysam Basiri. "Collaborative 3D Scene Reconstruction in Large Outdoor Environments Using a Fleet of Mobile Ground Robots". In: *Sensors* 23.1 (2022), p. 375.
- [18] Sean Bone et al. "Decentralised Multi-Robot Exploration using Monte Carlo Tree Search". In: *2023 IEEE/RSJ International Conference on Intelligent Robots and Systems (IROS)*. IEEE. 2023, pp. 7354–7361.
- [19] Daniel Strömbom et al. "Solving the shepherding problem: heuristics for herding autonomous, interacting agents". In: *Journal of the royal society interface* 11.100 (2014), p. 20140719.
- [20] Marco Dorigo, Mauro Birattari, and Thomas Stutzle. "Ant colony optimization". In: *IEEE computational intelligence magazine* 1.4 (2006), pp. 28–39.
- [21] Iain D Couzin et al. "Collective memory and spatial sorting in animal groups". In: *Journal of theoretical biology* 218.1 (2002), pp. 1–11.
- [22] William M Spears et al. "An overview of physicomimetics". In: *Swarm Robotics: SAB 2004 International Workshop, Santa Monica, CA, USA, July 17, 2004, Revised Selected Papers 1*. Springer. 2005, pp. 84–97.
- [23] Kelly J Benoit-Bird and Whitlow WL Au. "Cooperative prey herding by the pelagic dolphin, *Stenella longirostris*". In: *The Journal of the Acoustical Society of America* 125.1 (2009), pp. 125–137.
- [24] M Dorigo et al. "Influence of Leaders and Predators on Steering a Large-Scale Robot Swarm". In: *Swarm Intelligence: 11th International Conference, ANTS 2018, Rome, Italy, October 29–31, 2018, Proceedings*. Vol. 11172. Springer. 2018, p. 429.
- [25] Raghavv Goel et al. "Leader and predator based swarm steering for multiple tasks". In: *2019 IEEE international conference on systems, man and cybernetics (smc)*. IEEE. 2019, pp. 3791–3798.
- [26] Alireza Dirafzoon and Edgar Lobaton. "Topological mapping of unknown environments using an unlocalized robotic swarm". In: *2013 IEEE/RSJ International Conference on Intelligent Robots and Systems*. IEEE. 2013, pp. 5545–5551.
- [27] Jixuan Zhi and Jyh-Ming Lien. "Learning to herd agents amongst obstacles: Training robust shepherding behaviors using deep reinforcement learning". In: *IEEE Robotics and Automation Letters* 6.2 (2021), pp. 4163–4168.
- [28] Andrzej Reinke et al. "Locus 2.0: Robust and computationally efficient lidar odometry for real-time 3d mapping". In: *IEEE Robotics and Automation Letters* 7.4 (2022), pp. 9043–9050.
- [29] Matteo Palieri et al. "Locus: A multi-sensor lidar-centric solution for high-precision odometry and 3d mapping in real-time". In: *IEEE Robotics and Automation Letters* 6.2 (2020), pp. 421–428.
- [30] Tixiao Shan et al. "Lio-sam: Tightly-coupled lidar inertial odometry via smoothing and mapping". In: *2020 IEEE/RSJ international conference on intelligent robots and systems (IROS)*. IEEE. 2020, pp. 5135–5142.
- [31] Armin Hornung et al. "OctoMap: An efficient probabilistic 3D mapping framework based on octrees". In: *Autonomous robots* 34 (2013), pp. 189–206.
- [32] Matan Keidar and Gal A Kaminka. "Efficient frontier detection for robot exploration". In: *The International Journal of Robotics Research* 33.2 (2014), pp. 215–236.
- [33] PGCN Senarathne et al. "Efficient frontier detection and management for robot exploration". In: *2013 IEEE International Conference on Cyber Technology in Automation, Control and Intelligent Systems*. IEEE. 2013, pp. 114–119.
- [34] Trupti M Kodinariya, Prashant R Makwana, et al. "Review on determining number of Cluster in K-Means Clustering". In: *International Journal* 1.6 (2013), pp. 90–95.
- [35] Garima Jain and Bhawna Mallick. "A study of time series models ARIMA and ETS". In: *Available at SSRN 2898968* (2017).
- [36] Adebisi A Ariyo, Adewumi O Adewumi, and Charles K Ayo. "Stock price prediction using the ARIMA model". In: *2014 UKSim-AMSS 16th international conference on computer modelling and simulation*. IEEE. 2014, pp. 106–112.
- [37] Tomas Baca et al. "The MRS UAV system: Pushing the frontiers of reproducible research, real-world deployment, and education with autonomous unmanned aerial vehicles". In: *Journal of Intelligent & Robotic Systems* 102.1 (2021), p. 26.
- [38] Ji Zhang and Sanjiv Singh. "LOAM: Lidar Odometry and Mapping in Real-time." In: *Robotics: Science and Systems*. Berkeley, CA. 2014, pp. 1–9.